Catalysis Today 281 (2017) 101–108

Contents lists available at ScienceDirect

Catalysis Today

journal homepage: www.elsevier.com/locate/cattod

Reduction of nitrate by heterogeneous photocatalysis over pure and radiolytically modified TiO_2 samples in the presence of formic acid

Alexandre Hérissan[a], Jorge M. Meichtry[b,c], Hynd Remita[a], Christophe Colbeau-Justin[a], Marta I. Litter[b,c,d,*]

[a] Laboratoire de Chimie Physique, CNRS UMR 8000, Universiteí Paris-Sud, Universiteí Paris-Saclay, Bâtiment 349, 91405 Orsay, France
[b] Gerencia Química, Comisión Nacional de Energía Atómica, Av. Gral. Paz 1499, 1650 San Martín, Prov. de Buenos Aires, Argentina
[c] Consejo Nacional de Investigaciones Científicas y Técnicas, Godoy Cruz 2290, 1425, Ciudad Autónoma de Buenos Aires, Argentina
[d] Instituto de Investigación e Ingeniería Ambiental, Universidad de Gral. San Martín, Campus Miguelete, Av. 25 de Mayo y Francia, 1650 San Martín, Prov. de Buenos Aires, Argentina

ARTICLE INFO

Article history:
Received 15 March 2016
Received in revised form 13 May 2016
Accepted 14 May 2016
Available online 13 July 2016

Keywords:
Nitrate
TiO_2
Formic acid
Radiolytically modified TiO_2
Nitrite
Ammonium

ABSTRACT

Heterogeneous photocatalytic reduction of nitrate (2 mM) in the presence of formic acid (FA, 10 mM) using pure and modified TiO_2 samples under UV–vis irradiation was performed at pH 3, and the evolution of the intermediate and final products was analyzed. For this work, commercial samples (Evonik P25 and Cristal Global PC500 and PC10) were modified by γ-radiolysis with two noble metal nanoparticles known to behave differently in NO_3^- transformation, Ag and Pd. P25 was modified with Ag (0.5 and 2% w/w), while PC10 and PC500 were modified with Pd (1% w/w). The order of the photocatalytic activity of the materials for NO_3^- transformation was 2 Ag-P25 > PC500 > 0.5 Ag-P25 ≈ P25 ≫ 1 Pd-PC500 > PC10 > 1 Pd-PC10. Nitrite formation was observed in all cases but at low amounts, and its concentration was negligible (≤1 μM) after complete NO_3^- reduction. Ammonium was found as final product and remained in considerable amounts at the end of the irradiation. The nitrogen balance accounted for a large amount of non-identified nitrogen products formed during the photocatalytic reaction, probably N_2 or NO; this amount was higher for the P25 and PC500 pure samples. The efficiency on the use of FA as donor was evaluated and PC500 was found to be the most efficient sample in this sense. A mechanism is proposed to clarify the still not well understood process of TiO_2 heterogeneous photocatalytic transformation of nitrate, based on literature data and detected products.

1. Introduction

Nitrate is a water pollutant related to human activities, with particular impact in groundwaters and drinking water. NO_3^- ingestion causes high damage to health, as methemoglobinemia or stomach cancer, with high effect on the health of babies, as the "blue baby syndrome" or cyanosis. The WHO recommends a value of 50 mg L^{-1} as the maximum allowable concentration of NO_3^- in drinking water [1]. There are very well known treatments for NO_3^- removal, e.g., catalytic or electrochemical reduction, electrodialysis, distillation, biological degradation, ion exchange, reverse osmosis, etc. ([2] and references therein). However, more efficient alternatives are still imperative.

NO_3^- reduction in water can lead to several stable water soluble or volatile species like NO_2^-/HNO_2, nitrogen oxides (NO, NO_2, N_2O), nitroxyl (HNO), hydroxylamine (NH_2OH), hydrazine (N_2H_4), bimolecular nitrogen (N_2) or ammonium (NH_4^+), among others. However, the production of nontoxic forms should be preferred, as for example, transformation to molecular nitrogen. The presence of ammonia ($NH_4^+ + NH_3$) in waters, although of no direct importance for human health, might have indirect interference, for example in disinfection [3]. NO_2^-, more toxic than NO_3^-, should not be present, having a WHO guideline in drinking water of 3 mg L^{-1} [4].

NO_3^- removal from water by reductive heterogeneous photocatalysis with TiO_2 (HP) attracted the attention for almost 30 years ([2,5,6] and references therein). Recently, our group found for the first time that nitric oxide (NO) is one of the products of the photocatalytic reduction of NO_3^- in water using TiO_2 and formic acid (FA) as hole scavenger [7]. As very well established, after irradiation of TiO_2 with UV light, electrons are promoted from the valence band (VB) to the conduction band (CB) of the semiconductor, leav-

* Corresponding author at: Gerencia Química, Comisión Nacional de Energía Atómica, Av. Gral. Paz 1499, Buenos Aires 1650, Argentina.
E-mail addresses: marta.litter@gmail.com, litter@cnea.gov.ar (M.I. Litter).

http://dx.doi.org/10.1016/j.cattod.2016.05.044
0920-5861/

ing holes behind; an acceptor A can be photocatalytically reduced by TiO_2 CB electrons (e_{CB}^-) if its redox potential is more positive than that of the e_{CB}^-, and a donor D can be easily oxidized by VB holes (h_{VB}^+) if its redox potential is less positive than that of the h_{VB}^+ [8–10]. For the most used photocatalyst, Degussa P-25 (now Evonik AEROXIDE® P25), the values of the edges of CB and VB at pH 0 have been calculated as −0.3 and +2.9 V vs. SHE, respectively [11]. The processes can be described by Eqs. (S1)–(S11) (one-electron steps) shown in the Supporting Information (SI, Section S1) [2,8,12,13]. Generally, the conjugate anodic reaction is oxidation of water by h_{VB}^+, initiated by Eq. (S4) and ending in protons and oxygen. As Eq. (S9) is slow, reductions are generally improved by the addition of sacrificial agents, such as alcohols or carboxylic acids (RH), which form strong reducing species by oxidation by h_{VB}^+ or $HO^\bullet$ (Eq. (S10)). These generated intermediates promote also indirect reductions. Direct NO_3^- photocatalytic reduction by TiO_2 e_{CB}^- is not possible because the redox potential of NO_3^- to the radical anion ($E^0(NO_3^-/{}^\bullet NO_3^{2-}) = -0.89$ V)[1] [14,15] hinders e_{CB}^- attack [16]. Actually, poor reactivity for NO_3^- reduction or no reaction at all has been observed using bare TiO_2 in the absence of electron donors [2,5,16,17]. Therefore, a donor is required to allow indirect reduction through Eq. (S11); comparative studies have shown that, in general, FA is the best donor [18–22]. An enhancement of the efficiency for NO_3^- HP transformation has been observed in some cases with TiO_2 modified with nanoparticles of noble metals ([2,5] and references therein).

In this work, the efficiency of different TiO_2 samples, pure and radiolytically modified with Ag and Pd nanoparticles, have been compared in the NO_3^-/FA photocatalytic system. Solvent radiolysis is a powerful method to synthesize small and relatively monodisperse nanoparticles of controlled size and shape [23,24]. Although Pt has been very much studied as TiO_2 modifier in the NO_3^- reduction, Ag and Pd are less expensive and their study is relevant. A rather detailed mechanism of NO_3^- photocatalytic transformation is proposed, based on literature data and the identified products.

2. Experimental

2.1. Materials and methods

Commercial TiO_2 samples (Evonik AEROXIDE® P25 and CristalACTiV™ Millennium PC10 and PC500) were used as received. NO_3^- was used as KNO_3 (Merck, 99%) and FA was Carlo Erba (99%). For pH adjustments, dilute KOH (Biopack) was used. N_2 was 4.8 grade ([O_2] <4 ppm, Linde).

2.2. Synthesis of noble-metal nanoparticle modified TiO_2 samples

The modified TiO_2 samples were those prepared previously by radiolytic surface deposition of Ag and Pd nanoparticles [23,24]. Briefly, an ethanolic solution containing $AgClO_4$ was mixed with P25 in suspension, sonicated, degassed with N_2 and irradiated under stirring with a ^{60}Co panoramic gamma source of 3000 curies (dose rate = 2.3 kGy h^{-1}) [23]. The Pd-PC samples were prepared similarly using palladium (II) acetylacetonate and 2-propanol as the solvent [24]. The modified TiO_2 photocatalysts were separated by centrifugation and dried at 60 °C. The main physicochemical properties of the samples are summarized in Table 1.

Very small Ag nanoparticles, with homogeneous mean sizes ranging 1.3–2 nm, were deposited on the TiO_2 surface [23], whereas the Pd nanoparticles were slightly larger (mean size: 3.0 nm) [24].

Table 1
List and characteristics of the TiO_2 samples.

Sample	Composition	SSA[a] (m^2 g^{-1})	Particle size (nm)
P25 (Evonik)	80:20 anatase:rutile	50	25
0.5 Ag-P25	0.5 wt% Ag	49	ND
2 Ag-P25	2 wt% Ag	44	ND
PC500	anatase	317	5–10
Pd-PC500	1 wt% Pd	ND	ND
PC10	anatase[b]	10	65–75
Pd-PC10	1 wt% Pd	ND	ND

ND: not determined.
[a] SSA: BET specific surface area.
[b] The sintering temperature increases from PC500 to PC10 [25].

Although some properties on Table 1 have been not measured, it has been reported that the modification of the TiO_2 surface by small percentages of metals does not influence in a significant way the SSA or the particle size of the precursor [26,27].

2.3. Photocatalytic experiments

The experiments were performed using a commercial glass photoreactor immersion well (Photochemical Reactors Ltd.) provided with a medium pressure mercury lamp (125 W, $\lambda > 310$ nm, $\lambda_{max} = 365$ nm, other emissions at 408, 436 and 546 nm), surrounded by a water jacket set at 25 °C, acting simultaneously as IR filter. The incident photon flux per unit volume ($q^0_{n,p}/V$) on the wall of the irradiated cell, measured by potassium ferrioxalate, was 24 μeinstein s^{-1} L^{-1}.

A 200 mL suspension containing 2 mM NO_3^-, 10 mM FA and 200 mg TiO_2 was prepared. pH was adjusted to 3 and the suspension was sonicated for 2 min. 180 mL were poured into the reactor and kept under magnetic stirring in the dark for 30 min to ensure dark adsorption equilibrium. The remaining 20 mL were used to evaluate non photocatalytic changes in NO_3^- and FA concentration after 120 min of stirring in the dark; no changes were observed in any conditions. The lamp (warmed up during 30 min out of the setup) was put inside the reactor, and 2 mL samples were periodically taken. During the dark period and all throughout the run, N_2 was bubbled into the reactor at a flow rate of 0.3 L min^{-1}, to warrant anaerobic conditions. Each sample was first centrifuged and then filtered through a cellulose acetate membrane (Sartorius, 0.22 μm, 25 mm diameter) before analysis. Negligible changes on pH were observed at the end of all photocatalytic runs.

At least duplicate runs were performed for each condition, and the results were averaged, with relative standard deviations smaller than 5%. The fitting of the experimental points was made with Origin 8.0 software, with reduced χ^2 as the iteration-ending criterion.

2.4. Analysis

The NO_3^- and FA concentrations were measured by HPLC, following a previous reference [28] using an anion exchange column (Hamilton PRP X100, 250 × 4.6 mm) with 4 mM potassium biphthalate at pH 4.5 as the eluent, at 1 mL min^{-1} flow rate. A Cecil CE 4100 pump with a Cecil CE 4200 UV–vis detector (measurement at 295 nm) and a 50 μL injection loop were used. NO_2^- and NH_4^+ concentrations were followed spectrophotometrically according to Refs. [29] and [30], respectively.

3. Results and discussion

3.1. Conditions of the photocatalytic experiments

Photocatalytic reactions were carried out at pH 3, as NO_3^- reduction in the presence of FA is more effective in acid solutions,

[1] All redox potentials given in this work are standard values vs. SHE. Values correspond to those in homogeneous solutions, although reactions at the interface can be somewhat different.

according to the following global reactions for NH_4^+ and N_2 production, taken as examples [19,22]:

$$NO_3^- + 4HCOOH + 2H^+ \rightarrow 4CO_2 + NH_4^+ + 3H_2O \quad (1)$$

$$2NO_3^- + 5HCOOH + 2H^+ \rightarrow N_2 + 5CO_2 + 6H_2O \quad (2)$$

Also, at pH values below the pzc (6.4 for P25 [5,22]), the semiconductor surface is positively charged and facilitates NO_3^- adsorption. FA, upon adsorption on TiO_2, dissociates into $HCOO^-$ and H^+, which bind to low-coordinated Ti and O surface atoms, respectively [31]. Acid pH also favors FA adsorption; although at pH 3, 70% of FA is in the neutral form ($pK_a = 3.75$ [32]), the remaining formate (≈3 mM) is enough to saturate the P25 surface at 1 g L^{-1} loading [33].

According to Eqs. (1) and (2), reduction of one mole of NO_3^- to N_2 requires 2.5 mol of FA, while a complete reduction to NH_4^+ needs a molar ratio (MR) = 4. Therefore, the use of MR = 5 assures that FA will not be the limiting reagent; a higher FA amount would not increase the photocatalytic activity, due to a competition between NO_3^- and formate for the adsorption sites [18,19,34].

O_2 has to be eliminated [22,35,36] because it can compete with NO_3^- for the reducing agents present in the system [7].

3.2. Photocatalytic experiments with pure TiO_2 samples

The temporal evolution of NO_3^- normalized concentration during UV–vis irradiation of a 2 mM NO_3^- suspension in the presence of 10 mM FA and 1 g L^{-1} of pure TiO_2 samples at pH 3 is shown in Fig. 1(a). As observed, the order of reactivity was PC500 > P25 ≫ PC10. Fig. 1(b) shows the decay of FA normalized concentration.

A total disappearance of NO_3^- at 30 and 45 min is observed for PC500 and P25, respectively, while PC10 shows a low reactivity. The experimental data for NO_3^- could be fitted to a pseudo-first order rate law, according to Eq. (3):

$$\frac{[NO_3^-]}{[NO_3^-]_0} = A_1 \times \exp^{-k_1 \times t} + (1 - A_1) \quad (3)$$

where k_1 is the pseudo-first order kinetic constant for NO_3^- removal, and A_1 is the fraction of the initial NO_3^- that can be reduced. For all samples, $A_1 = 1$, indicating that a complete NO_3^- removal would be obtained with enough reaction time, even for PC10. Table S1 (Section S2) shows the fitting parameters. In previous photocatalytic studies, the temporal evolution of NO_3^- over P25 appeared as curved profiles with little sensitivity to either NO_3^- or hole scavenger concentration [5,35,37], but no kinetic equations have been tested in those works.

The experimental points for FA decay in our experiments could be fitted with Eq. (4):

$$\frac{[FA]}{[FA]_0} = \frac{A_2}{[FA]_0} \times \exp^{-k_2 \times t} + \left(1 - \frac{A_2}{[FA]_0}\right) \quad (4)$$

where k_2 has the same meaning as k_1 of Eq. (3), A_2 is the concentration of FA degraded during the photocatalytic experiment ($A_2 \leq 10$ mM), and $[FA]_0 = 10$ mM. The parameters are shown in Table S1. The photocatalytic FA degradation with O_2 at almost constant concentration showed a Langmuir-Hinshelwood kinetic behavior [38], which is not followed in the present anaerobic conditions, as FA could not be totally degraded over any photocatalyst because a complete depletion of acceptor species (i.e., NO_3^-, NO_2^- and other intermediates, see below) is reached before the end of the run for P25 and PC500. For these samples, the k_2 values are generally smaller than those of k_1, indicating that FA degradation continues even after complete NO_3^- removal by the action of some reducible intermediates.

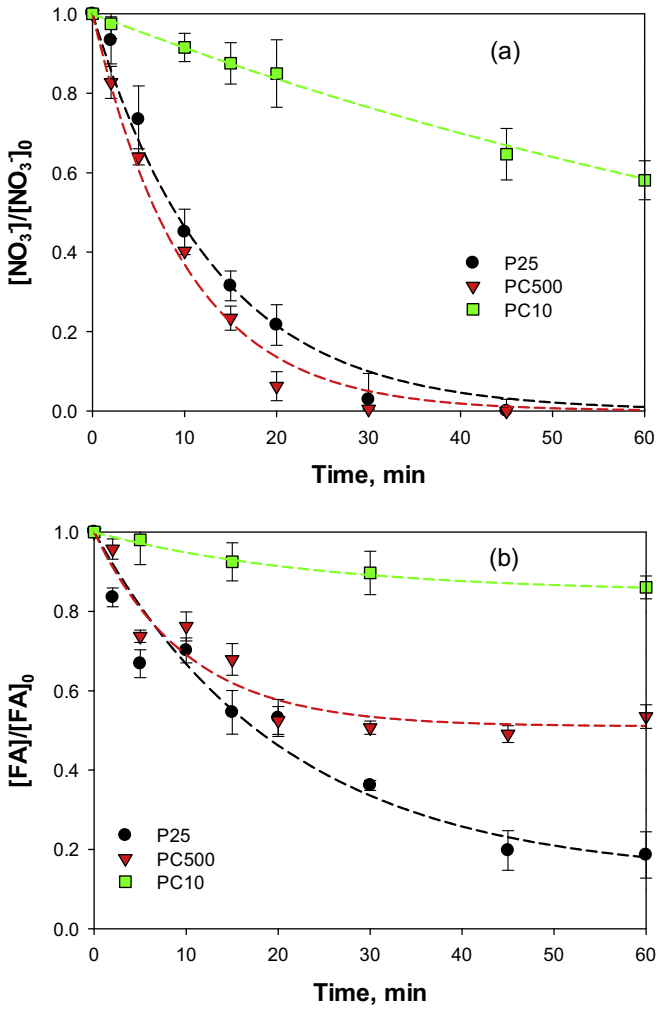

Fig. 1. Temporal evolution of (a) normalized NO_3^- concentration and (b) normalized FA concentration during the photocatalytic experiments with P25, PC500 and PC10. Conditions: $[NO_3^-] = 2$ mM, [FA] = 10 mM, $[TiO_2] = 1$ g L^{-1}, pH 3, T = 25 °C, λ > 310 nm, $\lambda_{max} = 365$ nm, $q^0_{n,p}/V = 24$ μeinstein s^{-1} L^{-1}. The dashed lines in (a) and (b) are the fittings of the experimental points using Eqs. (3) and (4), respectively.

It is important to state that Eqs. (3) and (4) have no theoretical footing, they are not connected to any chemical-physical parameters, and they are only phenomenological mathematical expressions, as good tools to fit the data.

Comparison of commercial TiO_2 samples indicated that PC10 was more active than PC500 for the treatment of species of low or null adsorption onto TiO_2, like phenol or rhodamine-B. This good performance of PC10 was explained because its manufacturing involves a thermal treatment that increases the particle size (Table 1) and the crystallinity of the sample, decreasing thus the rate of electron-hole recombination (e.g. [24,25,39]). In contrast, compounds that adsorb strongly, such as dichloroacetic, hydroxybenzoic or malic acids, are degraded more efficiently over materials with high SSA, as PC500 or P25. The higher activity of samples with high SSA in the HP NO_3^- transformation has been observed before [22], what explains the low activity of PC10 in the present case.

Comparing P25 and PC500, Fig. 1(a) and k_1 values (Table S1) indicate that PC500 is better than P25 for nitrate transformation; Fig. 1(b) and k_2 values indicate the same for FA degradation at short times, although at longer times total FA degradation is higher for P25 (see A_2 in Table S1). P25 has been found to be a better photocatalyst than pure anatase samples (e.g. Hombikat or Millennium) for the oxidation of organic compounds, when O_2 is the only or best

acceptor and the organic compound is not strongly adsorbed on the TiO_2 surface. This has been attributed to the unique structure of P25 having an anatase-rutile heterojunction [27,40]. In contrast, PC500 was found more active than P25 in two HP systems similar to that here studied (i.e., NO_3^- transformation in the presence of FA): reduction of Cr(VI) in the presence of EDTA [40] and reduction of Se(IV) and Se(VI) in the presence of FA [41]. In those cases, both donors and acceptors are strongly adsorbed on TiO_2, and large area samples (UV100, PC500) promote a high activity [39], enhanced by a decrease of the recombination rate in particles of size below 10 nm [42].

The A_2 values in Table S1 are always ≤10 mM, and this indicates that the amount of FA is enough; when complete NO_3^- reduction is obtained, A_2 can be used to compare the efficiency in the use of donor by the different photocatalysts: PC500 appears as the most efficient material in this sense.

As products of the HP treatment, NO_2^- ($pK_a = 3.3$ [43])[2] and NH_4^+ were identified and quantified in the aqueous phase. The rest of the possible products has been gathered as "non-identified nitrogen-containing products" (NINP), and their concentration was calculated from the mass balance using the experimental values of the effectively measured species at different times (t) (Eq. (5) [7]):

$$\mathrm{NINP} = [NO_3^-]_0 - [NO_3^-]_t - [NO_2^-]_t - [NO_4^+]_t \quad (5)$$

It can be assumed that NINP will correspond to gaseous compounds, e.g., N_2, NO_x and/or N_2O, purged from the reactor by the N_2 flow, and to water soluble compounds such as HNO ($pK_a = 11.4$ [44,45][3]) and NH_2OH (as NH_3OH^+, $pK_a = 5.93$ [46]). These products have been not analyzed in the present work. In Figs. S1(a), S1(b) and S1(c) of the SI (Section S2), the evolution of the concentration of NO_2^-, NH_4^+ and NINP, respectively, normalized to nitrate initial concentration, for the three pure samples is depicted. NH_4^+ concentration increased with rather similar conversions in all cases, but no total NO_3^- transformation to this product was obtained with any of the pure photocatalysts. NH_4^+ formation is arrested at around 30 min and remained almost unchanged until the end of the experiment. The observed induction period, much more important for PC10, suggests that the transformation of NO_3^- to NH_4^+ is not direct, but passes through several intermediates.

NO_2^- was formed at lower concentrations than NH_4^+ (cf. Figs. S1(a) and S1(b)). NO_2^- evolution shows a very rapid increase in the first minutes, followed by a total disappearance ($[NO_2^-] \leq 1\ \mu M$) for P25 and PC500 at the end of the run; $[NO_2^-]$ remains constant ($\cong 1\ \mu M$) after 5 min for PC10 (see Fig. S1(a), inset), reflecting an additional disadvantage of this photocatalyst, as this toxic pollutant is not totally removed, at least as long as nitrate is present in the system. Interestingly, a 10 times higher $[NO_2^-]$ was found for PC500 in the first minutes, but additional work has to be done to explain this behavior.

Fig. S1(c) shows normalized NINP evolution. The produced amount is higher than the $[NH_4^+]$ for the two best photocatalysts, PC500 and P25, reaching around 1.5 mM at 60 min from the 2 mM initial $[NO_3^-]$. The much higher $[NO_2^-]$ produced with PC500 in the first five min (Fig. S1(a)), which is not the case for the other pure TiO_2 samples, can be related with the maximum value of NINP observed at 20 min, i.e., 15 min after the NO_2^- peak and before the maximum concentration of NH_4^+ is attained. This suggests that part of these NINP are intermediates in the NO_2^- reduction to NH_4^+ that cannot be purged by the N_2 flow, for example, NH_2OH.

[2] According to the pK_a, at pH 3, nitrite can be present as NO_2^- or HNO_2, but for simplicity, it will be indicated as NO_2^- all throughout this text.

[3] Different values for this pK_a are reported but they are dependent on the spin state of the species. The value taken here corresponds to the singlet state.

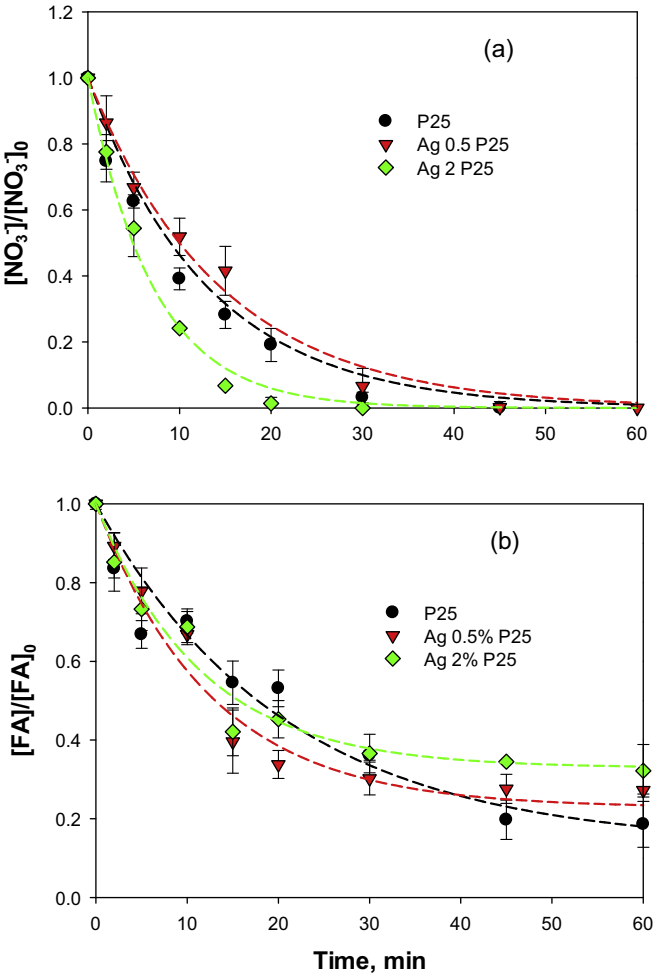

Fig. 2. Temporal evolution of (a) normalized NO_3^- concentration and (b) normalized FA concentration during the photocatalytic experiments with P25, 0.5 Ag-P25 and 2 Ag-P25. Same conditions of Fig. 1. The dashed lines are the fittings using Eqs. (3) and (4), respectively.

The fitting of the experimental points of the products or intermediates was not performed due to the complexity of the evolution seen in the figures.

The concentration of chemical species at 60 min and the selectivity of the reaction products are shown in Table S2 (Section S2). For P25 and PC500, the selectivity to NINP calculated as $[NINP]/([NO_3^-]_0-[NO_3^-]_t)$ at $t = 60$ min was high and very similar (77 vs. 72%, respectively), and significantly lower for PC10 (50%).

3.3. *Photocatalytic experiments with modified Ag-P25 samples*

Fig. 2 shows the temporal evolution of normalized $[NO_3^-]$ and [FA] for the Ag-modified P25 samples. The evolution of NO_2^-, NH_4^+ and NINP, normalized to nitrate initial concentration, is shown in Figs. S2(a), S2(b) and S2(c), respectively.

The 0.5 Ag-P25 sample was almost equally active as pure P25 for NO_3^- transformation, which was complete at 45 min, whereas 2 Ag-P25 was rather more efficient (Fig. 2(a)), the species totally disappearing at 30 min. The fitting parameters from Eqs. (3) and (4) are shown in Table S1 (Section S2). The k_1 values indicate that NO_3^- transformation is faster with the Ag-P25 samples compared with the precursor, especially with 2 Ag-P25. For FA degradation (Fig. 2(b)), all the modified samples behave similarly: an arrest is observed at around 20 min similarly to the case of PC500; P25 gives the highest FA degradation. However, the k_2 values are much higher

for the Ag-containing samples, and the A_2 values indicate that these samples require less FA to achieve a complete NO_3^- removal, being 2 Ag-P25 the most efficient. The same radiolytically prepared 0.5 and 2 Ag-P25 samples have been found to be more active than the pure precursor for phenol degradation [23]. This enhancement has been attributed to a Schottky barrier formation (~0.4 eV, as the work functions for Ag and P25 are 4.6 eV and 4.2 eV, respectively [19]), leading to a storage of electrons in the Ag(0) nanoparticles and a shift of the Fermi level [12]; besides, Ag nanoparticles induce NO_3^- reduction by e_{CB}^- [47]. The role of Ag nanoparticles coated on TiO_2 in enhancing the photocatalytic NO_3^- transformation has been reported before [16,18,19,34,47,48].

Toxic products as NO_2^- (Fig. 2(a)) and NH_4^+ (Fig. S2(b)) are produced over the two Ag-modified samples in higher amounts compared with P25. Again, as for the pure photocatalysts, some induction period is observed in NH_4^+ formation. All samples show a rapid initial NO_2^- formation with a maximum at 2 min and a complete disappearance after 15 min (Fig. S2(a) and Table S2). Noticeably, 2 Ag-P25 produced around 10 times more NO_2^- in the first minutes than the other two samples, as similarly observed by Gekko et al. for Ag–TiO_2 samples prepared by photodeposition [47]. No explanations can be proposed at present for this behavior.

The normalized evolution of NINP can be seen in Fig. S2(c); in all cases, the amount of these non-identified products at the end of the reaction is very important (>1.1. mM), but it was higher for the unmodified P25, the selectivity following the order P25 > 2 Ag-TiO_2 > 0.5 Ag-TiO_2 (Table S2), meaning that the incorporation of metals does not improve the production of the gaseous products, in contrast with the results obtained by other authors [17,34]. A rather similar result was obtained by Sá et al. [18] and by Gekko et al. [47], who found that an increase in the reactivity was not accompanied by a similar enhancement of the selectivity to gaseous products. Similarly to PC500, 2 Ag-P25 also shows a maximum NINP value, in this case at 15 min.

3.4. Photocatalytic experiments with modified PC samples

Fig. 3 shows the temporal evolution of NO_3^- and FA for the modified PC samples, while the normalized evolution of NO_2^-, NH_4^+ and NINP is shown in Fig. S3.

The Pd-modified samples showed an important decrease in the NO_3^- decay efficiency compared with the pure precursors (Fig. 3(a) and k_1 in Table S1): at 45 min, only PC500 yielded a complete NO_3^- disappearance. The pure PC10 sample, as said, shows a low reactivity due to their low SSA, which extends to Pd-PC10 (Table 1). In contrast, FA degradation at long times was enhanced by the presence of Pd (Fig. 3(b) and A_2 in Table S1), although at short times (<20 min), bare PC500 seems to be faster (k_2, Table S1). Alaoui et al. [24] found different results by the incorporation of Pd on PC samples, depending on the species to be degraded: the degradation of rhodamine B was enhanced, but for phenol, this effect was only observed using Pd-PC10, the modification being harmful for PC500. Pd modified samples consume more FA (A_2, Table S1) than the pure samples despite the decrease in the amount of NO_3^- reduced, i.e., there is a decrease in the donor efficiency, The increase in the amount of FA degraded cannot be ascribed to direct thermal oxidation of FA by Pd nanoparticles [49] because dark experiments (not shown) revealed negligible FA (and NO_3^-) transformation.

The deterioration of all processes by modification of PC samples with Pd (more noticeably for PC500), indicated by all kinetic parameters of Table S1, can be attributed to two main factors: 1) a blocking of the photocatalyst surface by the Pd nanoparticles and 2) a parallel H_2 formation competing with NO_3^- reduction [17,35].

Other results of Pd-modified TiO_2 samples for NO_3^- transformation [47,50–52] are variable and seem to be very dependent on the preparation and properties of the samples, turning the comparison very difficult.

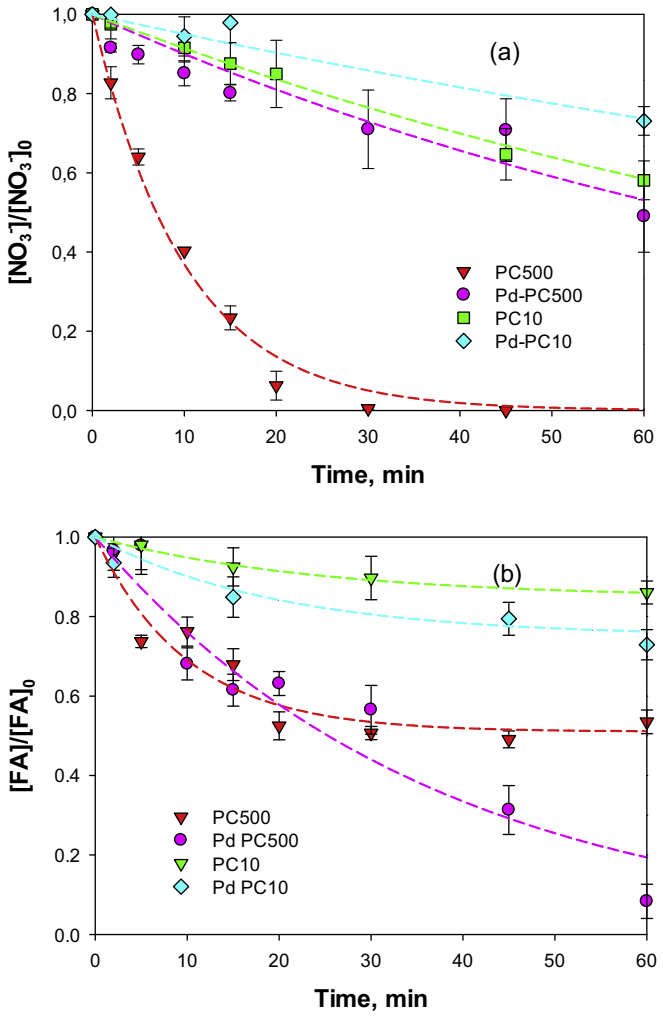

Fig. 3. Temporal evolution of (a) normalized NO_3^- concentration and (b) normalized FA concentration during the photocatalytic experiments with PC500, PC10, Pd-PC500 and Pd-PC10. Same conditions of Fig. 1. The dashed lines are the fittings using Eqs. (3) and (4), respectively.

NO_2^- (Fig. S3(a)) and NH_4^+ (Fig. S3(b)) were formed in lower amounts for the Pd PC500 sample, although the selectivity to NINP is much lower (56 vs. 72% for Pd PC500 and PC500, respectively, Table S2); for the PC10 samples, this difference is less significant and similar (46 vs. 50% for Pd PC10 and PC10, respectively, Table S2). The induction period for NH_4^+ formation is here rather visible for PC10 and Pd-PC10, but this is due surely to the low reactivity. At the end of the reaction (60 min), NO_2^- was not present in any of the Pd-modified systems, in contrast with PC10, where some minor amount still remained (Fig. S3(b)). However, an important NH_4^+ amount was found in all cases, even in the PC10 samples, of lower activity. Evolution of NINP (Fig. S3(c)) was only important for PC500, the results confirming the loss of photocatalytic efficiency for NO_3^- transformation due to Pd.

3.5. General mechanism for nitrate heterogeneous photocatalytic transformation over TiO_2

The photocatalytic mechanism of NO_3^- transformation is very complicated, consisting of consecutive and parallel steps, and involving several stable and unstable intermediates and products. We will propose a rather simplified mechanism (Table 2), but we

Table 2
Equations related to the proposed mechanism of nitrate reduction over TiO_2 photocatalyst under UV–vis irradiation.

Reaction	Thermodynamic and kinetic data	Refs.	Eq. number
$HCOO^- + h_{BV}^+ (HO^\bullet) \rightarrow H^+ + CO_2^{\bullet-} (+ OH^-)$			(6)
$CO_2^{\bullet-} + NO_3^- \rightarrow {}^\bullet NO_3^{2-} + CO_2$			(7)
${}^\bullet NO_3^{2-} + H_2O \rightleftarrows H^\bullet NO_3^- + OH^-$	$pK_a = 7.5$	[14,55]	(8)
$H^\bullet NO_3^- + H_2O \rightleftarrows H_2{}^\bullet NO_3 + OH^-$	$pK_a = 4.8$	[14]	(9)
$H^\bullet NO_3^-/H_2{}^\bullet NO_3 \rightarrow {}^\bullet NO_2 + OH^-/H_2O$		[14,55]	(10)
$2\ {}^\bullet NO_2 \rightleftarrows N_2O_4$	$k = 4.5 \times 10^8\ M^{-1}\ s^{-1}$	[14,55,56]	(11)
$N_2O_4 + H_2O \rightarrow NO_3^- + NO_2^- + 2\ H^+$	$k = 1 \times 10^3\ s^{-1}$	[56]	(12)
${}^\bullet NO_2 + e_{CB}^- (CO_2^{\bullet-}) \rightarrow NO_2^- (+ CO_2)$	$E^0(NO_2/NO_2^-) = 1.04\ V$	[63]	(13)
${}^\bullet NO_2 + HCOOH \rightarrow HNO_2 + CO_2^{\bullet-} + H^+$		[57]	(14)
$NO_2^- + CO_2^{\bullet-} \rightarrow {}^\bullet NO_2^{2-} + CO_2$	$E^0(NO_2^-/{}^\bullet NO_2^{2-}) = -0.47\ V$	[58]	(15)
$HNO_2 + e_{CB}^- (CO_2^{\bullet-}) \rightarrow {}^\bullet NO + OH^- (+CO_2)$	$E^0(HNO_2/{}^\bullet NO) = 0.875\ V$	[59]	(16)
$2\ HNO_2 \rightarrow {}^\bullet NO + {}^\bullet NO_2 + H_2O$			(17)
${}^\bullet NO_2^{2-} + NO_3^- \rightarrow NO_2^- + {}^\bullet NO_3^{2-}$			(18)
$NO_2^- + {}^\bullet NO_3^{2-} \rightleftarrows {}^\bullet NO_2^{2-} + NO_3^-$			(19)
${}^\bullet NO_2^{2-} + H_2O \rightleftarrows {}^\bullet NO + 2\ OH^-$			(20)
${}^\bullet NO + e_{CB}^- (CO_2^{\bullet-}) \rightarrow NO^- (+ CO_2)$	$E^0(NO/{}^3NO^-) = 0.39\ V$	[63]	(21)
$NO^- + H^+ \rightleftarrows HNO$	$pK_a = 11.4$	[44,45,64]	(22)
${}^\bullet NO + {}^\bullet NO_2 \rightleftarrows N_2O_3$	$k = 1.1 \times 10^9\ M^{-1}\ s^{-1}$	[56]	(23)
$N_2O_3 + H_2O \rightarrow 2\ NO_2^- + 2\ H^+$	$k = 5.3 \times 10^2\ s^{-1}$	[55]	(24)
$HNO + e_{CB}^- (CO_2^{\bullet-}) \rightarrow H_2NO^\bullet (+ CO_2)$	$E^0(HNO/H_2NO^\bullet) = 0.52\ V$	[76]	(25)
$2\ HNO \rightarrow N_2O + H_2O$			(26)
$HNO + 2\ {}^\bullet NO \rightarrow N_2O + HNO_2$		[45,55]	(27)
$N_2O + CO_2^{\bullet-} + H^+ \rightarrow N_2 + HO^\bullet (+ CO_2)$	$\Delta E^0(N_2O/N_2 + HO^\bullet) = -0.96\ V$[a]		(28)
$2\ H_2NO^\bullet \rightarrow N_2 + H_2O$		[64]	(29)
$H_2NO^\bullet + e_{CB}^- (CO_2^{\bullet-}) \rightarrow NH_2OH (+ CO_2)$	$E^0(H_2NO^\bullet/H_2NOH) = 0.90\ V$	[76]	(30)
$NH_2OH + H^+ \rightleftarrows NH_3OH^+$	$pK_a = 5.93$	[46]	(31)
$NH_3OH^+ + e_{CB}^- (CO_2^{\bullet-}) \rightarrow NH_3{}^{\bullet+} + OH^- (+ CO_2)$	$E^0(NH_3OH^+/NH_3{}^{\bullet+}) = -0.12\ V$	[63]	(32)
$NH_3{}^{\bullet+} \rightleftarrows NH_2{}^\bullet + H^+$	$pK_a = 2.3$	[63]	(33)
$2\ NH_2{}^\bullet \rightarrow N_2H_4$		[73]	(34)
$NH_2{}^\bullet + e_{CB}^- (CO_2^{\bullet-}) \rightarrow NH_2^- (+ CO_2)$	$E^0(NH_2{}^\bullet/NH_2^-) = 0.7\ V$	[63]	(35)
$NH_2^- + H^+ + H_2O \rightarrow NH_4OH$			(36)
$NH_2{}^\bullet + NH_3OH^+ \rightarrow NH_2^- + H_2NO^\bullet + H^+$		[73]	(37)
$NO_2^- + H^+ + h\nu\ (365\ nm) \rightarrow {}^\bullet NO + HO^\bullet$			(38)
$2\ HNO_2 \rightarrow {}^\bullet 4{}^\bullet NO + {}^\bullet NO_2 + H_2O$			(39)

[a] The calculation of this redox potential is in the SI, Section S3.

are conscious that other parallel reactions can occur. All stable gaseous products will be part of NINP, as indicated before.

In the Introduction section, it was said that direct e_{CB}^- reduction of NO_3^- is not possible because of the very negative redox potential of the $NO_3^-/{}^\bullet NO_3^{2-}$ couple. However, NO_3^- reduction is possible in the presence of FA, as the carboxyl radical ($CO_2^{\bullet-}$), a very strong reducing species ($E^0(CO_2/CO_2^{\bullet-}) \approx -2.0\ V$ [53], $pK_a = 1.4$ [54]), is generated (Eq. (6) [6]). Reduction (Eq. (7)) is followed by hydrolysis (Eqs. (8) and (9)), and decomposition to nitrogen dioxide (${}^\bullet NO_2$, Eq. (10)), reactions that are catalyzed at acid pH [14,15,55]. In the absence of other compounds, ${}^\bullet NO_2$ dimerizes very fast to N_2O_4 (Eq. (11)) [55,56], followed by a very fast disproportionation (Eq. (12)) [55,56], or reduction to NO_2^- by e_{CB}^- or $CO_2^{\bullet-}$ (Eq. (13)), or directly by FA (Eq. (14)) as proposed in the gas phase [58]. In the basic form, NO_2^- can be reduced to ${}^\bullet NO_2^{2-}$ by $CO_2^{\bullet-}$ (Eq. (15)) but not by e_{CB}^- [58]; however, at the working pH, the species is mainly as HNO_2, which can be reduced by both reductants [59] (Eq. (16)) or can slowly disproportionate (Eq. (17)), but this pathway can be neglected at low HNO_2 concentrations [60]. Although the oxidation of NO_2^- by h_{VB}^+ or $HO^\bullet$ is easy [55,61,], the presence of the high FA concentration avoids this reaction. ${}^\bullet NO_2^{2-}$ can react with NO_3^- (Eq. (18)) [55], although the back reaction (Eq. (19)) is also possible [58]. ${}^\bullet NO_2^{2-}$ can be also hydrolyzed to ${}^\bullet NO$ (Eq. (20)) [7,44,55,58]. Although dissimilar values of the redox potential of the ${}^\bullet NO/{}^3NO^-$ couple have been reported ($E^0 = -0.76\ V$ [62] and 0.39 V [45,63]), ${}^\bullet NO$ can be reduced to NO^- by $CO_2^{\bullet-}$ (which is as HNO at the working pH, Eqs. (21) and (22)); besides, Goldstein et al. [64] indicate that ${}^\bullet NO$ can be reduced by electrons generated in colloidal TiO_2. In addition, ${}^\bullet NO$ reacts very fast with ${}^\bullet NO_2$ to give N_2O_3 (Eq. (23)) [55,56], which is easily hydrolyzed, generating more NO_2^- (Eq. (24)) [43,55]. HNO can be reduced to the aminoxyl radical ($H_2NO^\bullet$) by e_{CB}^- or $CO_2^{\bullet-}$ (Eq. (25)), selfcombine to give N_2O (Eq. (26)) [45,55], or react with ${}^\bullet NO$ ending in N_2O and HNO_2 (Eq. (27)) [45,64,65]. The reactivity of N_2O toward e_{CB}^- is complex and the redox potential of the N_2O/N_2O^- couple is not known, as far as we know. Although the scavenging of e_{CB}^- by N_2O has been postulated over TiO_2 [66,67], it has been reported that this process is not efficient [64,68–70]. Nevertheless, N_2O may react with $CO_2^{\bullet-}$ to give N_2 plus $HO^\bullet$ (which will be rapidly scavenged by FA) (Eq. (28)) [71]. Recombination of $H_2NO^\bullet$ leads also to N_2 (Eq. (29)), but this is a minor pathway [64]. $H_2NO^\bullet$ can be reduced either by e_{CB}^- or $CO_2^{\bullet-}$ [72] to NH_2OH (protonated at pH 3 [46], Eqs. (30) and (31)), with further transformation to the aminyl radical ($NH_3{}^{\bullet+}/NH_2{}^\bullet$, Eqs. (32) and (33)) [56,64,73]. Although it has been reported that the one electron reduction of protonated NH_2OH (NH_3OH^+) gives NH_3 plus $HO^\bullet$ [63], the reduction potential is rather negative ($E^0 = -0.58\ V$); however, Goldstein et al. reported that NH_2OH at pH 2 does react with trapped e_{CB}^-, suggesting the occurrence of other reaction pathways. $NH_2{}^\bullet$ can dimerize to N_2H_4 (Eq. (34)) [73] or can be reduced by e_{CB}^- or $CO_2^{\bullet-}$ to NH_2^- (as NH_4^+ at pH 3, Eqs. (35) and (36)), or oxidize NH_2OH (Eq. (37)) [73].

Other reactions as those between HNO or NO with NH_2OH [45] or between NO_2^- and NH_4^+ to N_2 [74] can be considered negligible according to the values of the reaction rates. Photolytic reactions (38) and (39) [7] are also feasible; however, under the studied conditions, most of the UV-A light will be absorbed by TiO_2.

N_2 has been proposed as a product of NO_3^- transformation over P25, and several authors [5,18,22,34] indicate different selectivities. However, none of them have actually measured N_2, although the quantification of N_2 emissions has been reported with P25 modified with Ag [34] and Pd-Cu [17], and with Pt-P25 plus SnPd/Al_2O_3 [78]. In addition, although N_2 can be produced, its catalytic reduction to other products is extraordinarily difficult because it binds weakly to solid-state catalysts and the reaction involves high-energy inter-

mediates [75]. Considering that $^{\bullet}NO_2$, N_2O_4 and N_2O_3 are very soluble and unstable in aqueous solution [43], the contribution of these species to NINP is negligible, being only NO, N_2O and N_2 the main gaseous contributing species.

The above mechanism pathways are supported by the work of Goldstein et al. [64] where $^{\bullet}NO$ reduction either to NH_3 via five consecutive one-electron transfer reactions, involving NH_2OH formation, or to N_2 and/or N_2O through a parallel pathway are well described.

3.6. Effect of modification of TiO_2 with Ag and Pd on the photocatalytic mechanism

In the case of the metal modified TiO_2 (Ag and Pd), as said before, a Schottky barrier is formed, which inhibits the electron-hole recombination and improves the photocatalytic NO_3^- transformation [8]. Metals in the zerovalent state (M(0)) can allow also the photocatalytic production of H_2 by e_{CB}^- reduction of protons to hydrogen atoms ($H^{\bullet}$), a thermodynamically unfeasible process over pure TiO_2 ($E^0(H^+/H^{\bullet}) = -2.3$ V [77]), but more possible when metals are present (Eq. (40)). When FA is present, the produced carboxyl radical has different ways of decay: it can inject electrons to the TiO_2 CB, Eq. (41) (current-doubling effect) or transfer an electron to $H^+(M(0))$, generating also $H^{\bullet}$, Eq. (42) [6]. $H^{\bullet}$ combination generates H_2 (Eq. (43)).

$$H^+(M(0)) + e_{CB}^- \rightarrow H^{\bullet}(Me(0)) \quad (40)$$

$$CO_2^{\bullet -} \rightarrow CO_2 + e_{CB}^- \quad (41)$$

$$CO_2^{\bullet -} + H^+(M(0)) \rightarrow H^{\bullet}(Me(0)) + CO_2 \quad (42)$$

$$2\,H^{\bullet}(M(0)) \rightarrow H_2 \quad (43)$$

It was claimed that H_2 and $H^{\bullet}$ might provide an additional way of NO_3^- reduction [19,78], but the effect remained unclear. In fact, this process competes with NO_3^- reduction, the selectivity being determined by the hydrogen overpotential (HOV) of the loaded metal [17,79]. Ag has a large HOV (0.30 V), whereby H_2 production is inhibited, as the metal provides active sites for NO_3^- reduction [16,47,80]. In contrast, Pd [81], does not provide these active sites for NO_3^-, and its low HOV (0.04 V) [47] makes more feasible H_2 production (e.g. [2,82]).

When $^{\bullet}H$ formation is expected (Eq. (40)), transformation of NO to HNO according to reaction (44) is also possible [83]:

$$^{\bullet}NO + H^{\bullet} \rightarrow HNO \quad (44)$$

This, in turn, would favor the formation of NH_4^+ through Eqs. (25) and (30)–(36); the decrease in the selectivity to NINP observed using both metal-modified samples supports this mechanism. Another possibility for this decrease is related to the reported strong adsorption of NO on Pd [81,84], from where it can be reduced to N_2, N_2O, NH_2OH and/or NH_3, depending on the $[H^{\bullet}]$ and $[NO_2^-]$, with high $H^{\bullet}/NO_2^-$ ratios favoring the reduction to NH_3. With the Pd samples, $[NO_2^-]$ is always very low (see Fig. S3(a)), explaining the smaller NINP yields obtained with the Pd-PC samples. Besides, the photocatalytic formation of H_2 (Eq. (43)) is expected due the low HOV of Pd, which competes with NO_3^- reduction [2,16,17,47]. This is consistent with the increase of the consumption of FA observed in the experiments with these Pd-modified samples.

4. Conclusions

Photocatalytic experiments for NO_3^- reduction have been driven using different pure titania and radiolytically Ag and Pd modified samples. The order of the photocatalytic activity of the materials for NO_3^- reduction (according to the temporal profiles) was 2 Ag-P25 > PC500 > 0.5 Ag-P25 ≈ P25 ≫ Pd-PC500 > PC10 > Pd-PC10. Regarding FA decomposition, the activity was somewhat different: PC500 > 2 Ag-P25 > 0.5 Ag-P25 > Pd-PC10 ≅ P25 > PC10 > Pd-PC500, although it should be considered that different amounts of FA are consumed. PC500 was the sample that required the smallest amount of FA to completely reduce nitrate. A first order rate regime was found for the temporal NO_3^- and FA decay in all cases.

NO_2^- and NH_4^+ were formed with all the samples. NO_2^- was totally consumed but NH_4^+ remained in solution in considerable amounts. However, NINP (probably NO, N_2O and N_2) were found in all cases in rather high amounts, at higher or at least at similar concentrations than NH_4^+ (Table S2). The order for the selectivity to NINP formation was P25 > PC500 > 2 Ag-P25 > 0.5 Ag-P25 ≈ Pd-PC500 > PC10 > Pd-PC10. The case of 2 Ag-P25 is important: although it shows a high activity for NO_3^- removal, a significant increase in the amount of NO_2^- (transient) and of NH_4^+ was obtained, together with a lower selectivity to NINP formation. The modification of P25 with lower amounts of Ag was not effective to improve the activity.

The modification of PC samples with Pd deteriorates NO_3^- transformation and decreases significantly the efficiency in the use of the donor, most probably due to competence of H_2 evolution.

It can be concluded that the radiolytic modification of TiO_2 with noble metal nanoparticles such as Ag or Pd does not always increase the photocatalytic efficiency of NO_3^- reduction. The reasons for this differential behavior are related to the inherent mechanism of nitrate degradation and the possible side reactions that can be involved, such as H_2 generation.

A mechanism for HP transformation of NO_3^-, explaining the formation of the detected species is proposed. This mechanism should be improved by other experimental evidences that are underway.

Acknowledgements

This work was performed as part of A11E05ECOS/MINCyT collaborative project, and Agencia Nacional de Promoción Científica y Tecnológica PICT-512, PICT-0463 and PIP-CONICET 11220110100467 projects.

Appendix A. Supplementary data

Supplementary data associated with this article can be found, in the online version, at http://dx.doi.org/10.1016/j.cattod.2016.05.044.

References

[1] WHO, Guidelines for Drinking-water Quality, 2011, pp. 398–403, Available at: http://http://whqlibdoc.who.int/publications/2011/9789241548151_eng.pdf (last accessed 12.10.15).
[2] M.I. Litter, N. Quici, J.M. Meichtry, A. Senn, Photocatalytic removal of metallic and other inorganic pollutants, in: J. Schneider, D. Bahnemann, J. Ye, G. Li Puma, D. Dionysiou (Eds.), Photocatalysis: Fundamentals and Perspectives, The Royal Society of Chemistry, Cambridge CB4 0WF, UK, 2015, Chap. 5. ISBN 9781782620419.
[3] WHO/SDE/WSH/03.04/01, World Health Organization 2003, Ammonia in drinking-water, background document for development of WHO Guidelines for Drinking-water Quality.
[4] WHO/SDE/WSH/07.01/16/Rev/1. Nitrate and nitrite in drinking-water. Background document for development of WHO Guidelines for Drinking-water Quality Nitrate and Nitrite in Drinking, World Health Organization, 2011.
[5] M. Shand, J.A. Anderson, Catal. Sci. Technol. 3 (2013) 879.
[6] L.L. Perissinotti, M.A. Brusa, M.A. Grela, Langmuir 17 (2001) 8422.
[7] V.N. Montesinos, N. Quici, H. Destaillats, M.I. Litter, RSC Adv. 5 (2015) 85319.
[8] A.L. Linsebigler, G. Lu, J.T. Yates Jr., Chem. Rev. 95 (1995) 735.
[9] M.R. Hoffmann, S.T. Martin, W. Choi, D. Bahnemann, Chem. Rev. 95 (1995) 69.
[10] K. Nakata, A. Fujishima, J. Photochem. Photobiol. C 13 (2012) 169.
[11] S.T. Martin, H. Herrmann, M.R. Hoffmann, J. Chem. Soc. Faraday Trans. 90 (1994) 3323.

[12] P.V. Kamat, J. Phys. Chem. Lett. 3 (2012) 663.
[13] M.I. Litter, Adv. Chem. Eng. 36 (2009) 37.
[14] R.W. Fessenden, D. Meisel, J. Am. Chem. Soc. 122 (2000) 3773.
[15] A.R. Cook, N. Dimitrijevic, B.W. Dreyfus, D. Meisel, L.A. Curtiss, D.M. Camaioni, J. Phys. Chem. A 105 (2001) 3658.
[16] B. Ohtani, M. Kakimoto, H. Miyadzu, S. Nishimoto, T. Kagiya, J. Phys. Chem. 92 (1988) 5773.
[17] H. Kominami, T. Nakaseko, Y. Shimada, A. Furusho, H. Inoue, S.-Y. Murakami, Y. Kera, B. Ohtani, Chem. Commun. 3 (2005) 2933.
[18] J. Sá, C.A. Agüera, S. Gross, J.A. Anderson, Appl. Catal. B: Environ. 85 (2009) 192.
[19] A.V. Lozovskii, I.V. Stolyarova, R.V. Prikhod'ko, V.V. Goncharuk, J. Water Chem. Technol. 31 (2009) 360.
[20] K. Doudrick, O. Monzón, A. Mangonon, K. Hristovski, P. Westerhoff, J. Environ. Eng. 138 (2012) 852.
[21] K. Doudrick, T. Yang, K. Hristovski, P. Westerhoff, Appl. Catal. B: Environ. 136 (2013) 40.
[22] O.S.G.P. Soares, M.F.R. Pereira, J.J.M. Órfão, J.L. Faria, C.G. Silva, Chem. Eng. J. 251 (2014) 123.
[23] E. Grabowska, A. Zaleska, S. Sorgues, M. Kunst, A. Etcheberry, C. Colbeau-Justin, H. Remita, J. Phys. Chem. C 117 (2013) 1955.
[24] O.T. Alaoui, A. Herissan, C. Le Quoc, M.M. Zekri, S. Sorgues, H. Remita, C. Colbeau-Justin, J. Photochem. Photobiol. A 242 (2012) 34.
[25] A.G. Agrios, P. Pichat, J. Photochem. Photobiol. A 180 (2006) 130.
[26] E. Kowalska, H. Remita, C. Colbeau-Justin, J. Hupka, J. Belloni, J. Phys. Chem. C 112 (2008) 1124.
[27] C.A. Emilio, M.I. Litter, M. Kunst, M. Bouchard, C. Colbeau-Justin, Langmuir 22 (2006) 3606.
[28] P.A. Babay, C.A. Emilio, R.E. Ferreyra, E.A. Gautier, R.T. Gettar, M.I. Litter, Water Sci. Technol. 44 (2001) 179–185.
[29] Standard Methods 4500-NO2-B, Colorimetric Method, in Standard methods for the examination of water and wastewater, APHA, AWWA, and WEF, Editors, 2005.
[30] Standard Methods 4500-NH3F. Phenate Method, in Standard methods for the examination of water and wastewater, APHA, AWWA and WEF, Editors, 2005.
[31] A. Mattsson, S. Hu, K. Hermansson, L. Österlund, J. Chem. Phys. 140 (2014) 034705.
[32] E.V. Anslyn, D.A. Dougherty, Modern Physical Organic Chemistry, University Science Books, Sausalito, California, 2006, pp. 285.
[33] N. Serpone, J. Martin, S. Horikoshi, H. Hidaka, J. Photochem. Photobiol. A: Chem. 169 (2005) 235.
[34] F. Zhang, R. Jin, J. Chen, C. Shao, W. Gao, L. Li, N. Guan, J. Catal. 232 (2005) 424.
[35] J.A. Anderson, Catal. Today 175 (2011) 316.
[36] D.D.B. Luiz, S.L.F. Andersen, C. Berger, H.J. José, R.D.F.P.M. Moreira, J. Photochem. Photobiol. A: Chem. 246 (2012) 36.
[37] J.A. Anderson, Catal. Today 181 (2012) 171.
[38] A.R. Tôrres, E.B. Azevedo, N.S. Resende, M. Dezotti, Brazilian J. Chem. Eng. 24 (2007) 185.
[39] D. Gumy, S.A. Giraldo, J. Rengifo, C. Pulgarin, App. Catal. B 78 (2008) 19.
[40] J.M. Meichtry, C. Colbeau-Justin, G. Custo, M.I. Litter, Appl. Catal. B 144 (2014) 189.
[41] V.N.H. Nguyen, R. Amal, D. Beydoun, Chem. Eng. Sci. 60 (2005) 5759.
[42] M. Anpo, T. Shima, S. Kodama, Y. Kubokawa, J. Phys. Chem. 91 (1987) 4305.
[43] S.E. Schwartz, W.H. White, in: J.R. Pfafflin, E.N. Ziegler (Eds.), Adv. Environ. Sci. Eng., vol. 4, Gordon and Breach Science Publishers, 1981.
[44] V. Shafirovich, S.V. Lymar, Proc. Natl. Acad. Sci. U. S. A. 99 (2002) 7340.
[45] K.M. Miranda, Coord. Chem. Rev. 249 (2005) 433.
[46] J. Mollin, F. Kašpárek, J. Lasovský, Chem. Zvesti 29 (1975) 39.
[47] H. Gekko, K. Hashimoto, H. Kominami, Phys. Chem. Chem. Phys. 14 (2012) 7965.
[48] K. Kobwittaya, S. Sirivithayapakorn, J. Saudi Chem. Soc. 18 (2014) 291.
[49] W.P. Zhou, A. Lewera, R. Larsen, R.I. Masel, P.S. Bagus, A. Wieckowski, J. Phys. Chem. B 110 (2006) 13393.
[50] A. Kudo, K. Domen, K. Maruya, T. Onishi, Chem. Lett. (1987) 1019.
[51] W. Gao, R. Jin, J. Chen, X. Guan, H. Zeng, F. Zhang, N. Guan, Catal. Today 90 (2004) 331.
[52] K.T. Ranjit, B. Viswanathan, J. Photochem. Photobiol. A 108 (73) (1997) 73.
[53] P. Wardman, J. Phys. Chem. Ref. Data 18 (1989) 1637.
[54] G.V. Buxton, R.M. Sellers, J. Chem. Soc. Faraday Trans. 1 (1973) 555.
[55] M.C. Gonzalez, A.M. Braun, Res. Chem. Intermed. 21 (1995) 837.
[56] M.C. Gonzalez, A.M. Braun, J. Photochem. Photobiol. A 93 (1996) 7.
[57] F.H. Pollard, K.A. Holbrook, Trans. Faraday Soc. 53 (1957) 468.
[58] D. Meisel, Interim Report, U.S. Department of Energy, 1999 (http://digital.library.unt.edu/ark:/67531/metadc786966/m2/1/high_res_d/pdf (accessed 19.01.15).
[59] M.S. Ram, D.M. Stanbury, J. Am. Chem. Soc. 106 (1984) 8136.
[60] Q. Cai, W. Zhang, Z. Yang, Anal. Sci. 17 (2001) i917.
[61] J.A. Navío, G. Colón, A.M. Trillas, J.A. Peral, X. Domènech, J.J. Testa, J. Padrón, D. Rodríguez, M.I. Litter, Appl. Catal. B 16 (1998) 187.
[62] M.D. Bartberger, W. Liu, E. Ford, K.M. Miranda, C. Switzer, J.M. Fukuto, P.J. Farmer, D.A. Wink, K.N. Houk, Proc. Natl. Acad. Sci. U. S. A. 99 (2002) 10958.
[63] D.M. Stanbury, Adv. Inorg. Chem. 33 (1989) 69.
[64] S. Goldstein, D. Behar, T. Rajh, J. Rabani, J. Phys. Chem. A 119 (2015) 2760.
[65] S.V. Lymar, V. Shafirovich, G.A. Poskrebyshev, Inorg. Chem. 44 (2005) 5212.
[66] M. Anpo, N. Aikawa, Y. J. Chem. Soc. Kubokawa, Chem. Commun. (1984) 644.
[67] V. Sukharev, R. Kershaw, J. Photochem. Photobiol. A 98 (1996) 165.
[68] N. Serpone, P. Maruthamuthu, P. Pichat, E. Pelizzetti, H. Hidaka, J. Photochem. Photobiol. A 85 (1995) 247.
[69] J. Lee, H. Park, W. Choi, Environ. Sci. Technol. 36 (2002) 5462.
[70] H. Liao, T. Reitberger, Catalysts 3 (2013) 418.
[71] M.I. Al-Sheikhly, H.-P. Schuchmann, C. von Sonntag, Int. J. Rad. Biol. 47 (1985) 457.
[72] P. Neta, R.E. Huie, A.B. Ross, J. Phys. Chem. Ref. Data 17 (1988) 1027.
[73] M. Simic, E. Hayon, J. Am. Chem. Soc. 93 (1971) 5982.
[74] T.L. Brown, H.E. LeMay Jr., C. Bursten, P. Murphy, S. Woodward, D. Langford, A. George, Chemistry: The Central Science, 3rd ed., Pearson Higher Education AU, 2013, pp. 572, https://books.google.com.ar/books?id=zSziBAAAQBAJ&pg=PA571&lpg=PA571&dq=9781442554603+NO2-+%2B+NH4%2B&source=bl&ots=xLyEmmX9Bl&sig=Q1-Enu1k_f-eLjmkpdy_iq_XAchI=essa=Xved=0ahUKEwj1xZuEkfPKAhUJFJAKHVb3DzgQ6AEIGzAA#v=onepage&q=9781442554603%20NO2-%20%2B%20NH4%2B&f=false (accessed 13.02.16).
[75] D. Zhu, L. Zhang, R.E. Ruther, R.J. Hamers, Nature Mater, published on line 30-June-2013, 10.1038/NMAT3696.
[76] J. Lind, G. Merenyi, J. Phys. Chem. A 110 (2006) 1927.
[77] M. Breitenkamp, A. Henglein, J. Lilie, Ber. Bunsen-Ges. 80 (1976) 973.
[78] J. Hirayama, Y. Kamiya, ACS Catal. 4 (2014) 2207.
[79] H. Gekko, K. Hashimoto, H. Kominami, Phys. Chem. Chem. Phys. 14 (2012) 7965.
[80] H. Kominami, H. Gekko, K. Hashimoto, Phys. Chem. Chem. Phys. 12 (2010) 15423.
[81] M. Duca, B. van der Klugt, M.T.M. Koper, Electrochim. Acta 68 (2012) 32.
[82] J. Hirayama, H. Kondo, Y. Miura, R. Abe, Y. Kamiya, Catal. Commun. 20 (2012) 99.
[83] N. Wehbe, M. Jaafar, C. Guillard, J.-M. Herrmann, S. Miachon, E. Puzenat, N. Guilhaume, Appl. Catal. A 368 (2009) 1.
[84] H. Shin, S. Jung, S. Bae, W. Lee, H. Kim, Environ. Sci. Technol. 48 (2014) 12768.